

Modelling and Predicting of the Characteristics of a Photovoltaic Generator on a Horizontal and Tilted Surface

Mustapha Elyaqouti¹, Lahoussine Bouhouch², Ahmed Ihlal³

^{1,2}ERTAIER, ESTA Ibn Zohr University, BP 33/S, 80000 Agadir, Morocco

³LMER, FS Ibn Zohr University, BP 8106, 80000 Agadir, Morocco

Article Info

Article history:

Received Jul 4, 2016

Revised Oct 19, 2016

Accepted Nov 2, 2016

Keyword:

Kasten model

Prediction

PVG modeling

Solar radiation

ABSTRACT

In the present paper, we will attempt to predict the I_{pv} - V_{pv} output characteristic of a photovoltaic generator (PVG) and consequently the generated electric power. This will be possible through modeling, extracting the electrical parameters of the PVG under study and also, by estimating the global incident solar radiation, on a surface, first horizontally, and then tilted to a given angle. Mathematical models developed in Matlab, to characterize the studied PVG are validated by experimental data of the PVG manufacture. While models associated with global radiation are validated by measurements taken by the meteorological station installed on the laboratory site ERTAIER (Team for Research in Technology and Advanced Engineering of Renewable Energies) of Higher School of Technology Agadir (ESTA).

Copyright © 2016 Institute of Advanced Engineering and Science.

All rights reserved.

Corresponding Author:

Mustapha Elyaqouti,
ERTAIER, ESTA Ibn Zohr University,
BP 33/S, 80000 Agadir, Morocco.
Email: elyaqouti@gmail.com

1. INTRODUCTION

Solar energy is recognized as a promising alternative solution to the problems of fossil fuel depletion and global warming. We have witnessed in the last decade that Renewable Energies are providing more and more significant part in the energy mix in some countries. Photovoltaic conversion (PV), for instance, is expected to play a major role in electricity supply. Solar PV is covering more than 7 % of the electricity demand in many countries in Europe. By 2050, PV's share of global electricity is expected to reach 16%. However, the intermittency of solar impacts on security of energy supply.

Thus, the accurate modeling of photovoltaic generators is a major concern because it allows the designer to optimize performance and maximize the profitability of such PV systems [1].

The study of the PV functioning systems in steady state requires the development of models to estimate the amount of energy to be produced by a given PV system. These models are classified into two types: First, those that model the efficiency of a PVG, usually based on a direct expression for estimating the maximum power of PVG. The Second are those that model the current and voltage of the module and consequently the electrical power supplied by the PVG [2]. This modeling is typically used to approximate the output of PVG according to the two inputs that are solar radiation and module temperature, which is none other than the operating temperature of the photovoltaic cells [3]. However, the needed data are not available on all sites, for this reason, we have to use some approximate methods for predicting incident solar radiation on a horizontal surface or tilted at a given angle.

In this work, we propose an approach that allows the prediction of the output characteristics I_{pv} - V_{pv} of a given PV module for different inclinations. This will permit us then, the deduction of the maximum power generated by the PV module under study at any time and any day of the year.

The block diagram of the model we have developed in Matlab is shown in Figure 1. Our model

calculates the G incident solar irradiance on a horizontal surface, while calculating the direct solar irradiance G_{dir} and diffuse G_{diff} . Once it has been given the day number n , hour h or True Solar time (TST) and geographical coordinates of the place, given by latitude φ , longitude L and altitude Z . From the values of G_{dir} and G_{diff} , we can determine the value of the incident solar radiation G_{β} on an β angle tilted surface. After this phase, the knowledge of G_{β} and cells temperature T_{cell} are sufficient to the prediction of the output characteristic I_{pv} - V_{pv} , and therefore the simulated maximum power $P_{max,s}$ of the studied PVG.

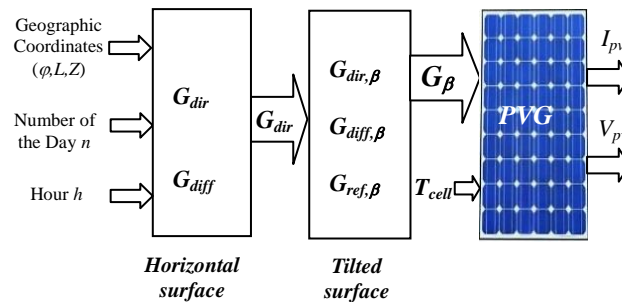


Figure 1. Diagram Block of Developed Model

Our paper is organized as follows: after an introduction, Section 2 describes the site concerned by the used meteorological measurements. Section 3 discusses the modelling of the incident solar radiation on horizontal and/or tilted surfaces. Then, we present in section 4 the modelling and characterization of the studied PVG. A conclusion and future prospects are presented at the end of this document.

2. SITE AND METEOROLOGICAL MEASUREMENTS

The meteorological data such as direct and diffuse solar radiation, ambient temperature, humidity and the wind speed and direction are collected by various sensors connected to a *Campbell* data logger CRX10X installed at the *ERTAIER* Laboratory at the higher school of technology (*ESTA*) Agadir (Figure 2). The data are collected every 10 seconds. They can be presented in different formats: average, min, max, etc., according to the chooses configuration in the data logger [4-5]. The data used in this work are related to Agadir site for which the geographical coordinates are:

- Longitude $\varphi = 9.579^{\circ}W$,
- Latitude $L = 30.406^{\circ}N$ and
- Elevation $Z = 41$ m.



Figure 2. Meteorological Station *Campbell* Data Logger CRX10X

3. SOLAR RADIATION MODELING

In this section, we present the procedure for modeling the incident solar radiation on a horizontal surface first and then β angle tilted. To achieve this, we will discuss the theory of atmospheric and geometric parameters used to estimate the solar radiation.

3.1. Atmospheric and Geometric Parameters Modeling

3.1.1. Earth Geographic Coordinates

These celestial ecliptic coordinates, are angular coordinates that identify a point or a place on the earth. It is a three coordinate system which are: the latitude, longitude and altitude. This coordinate system is shown in Figure 3.

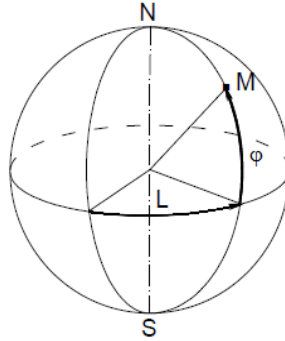


Figure 3. Earth geographic coordinates

3.1.1.1. Latitude ϕ

It is the angle between the equator plane and the direction connecting the center of the earth at the considered point. Its value is positive in the northern hemisphere while it is negative in the southern hemisphere [6].

3.1.1.2. Longitude L

It is the angle that the local meridian, passing through the point in question, with the meridian of origin, passing through the town of Greenwich. Its value is positive in the West while it is negative in the east of the origin meridian [7].

3.1.1.3. Altitude Z

It is the elevation of a location above the sea level, measured in meters.

3.1.2. Locating the Sun Position

The apparent movement of the sun is the movement that seems, to be done in a day, by the sun for an observer on the Earth installed outside the polar regions [8]. The apparent position of the sun is identified, every moment on the day and a year by two different coordinate systems: The hours celestial coordinate and horizontal celestial coordinates [9].

3.1.2.1. The Hours Celestial Coordinate

a) Sun Declination δ

The declination δ is the angle formed by the direction Earth-Sun relative to the Earth's equator [10]. It is expressed in degrees ($^{\circ}$), in minute ($'$) and seconds ($''$). This angle varies very little within a day and its value ranges from -23.45° at the winter solstice and $+23.47^{\circ}$ at the summer solstice and it is zero at the equinoxes of spring and autumn. It is calculated by the following equation [11]:

$$\delta = 23.45 \sin \left[360 * (284 + n) / 365.25 \right] \quad (1)$$

b) Hour Angle of the Sun H

This is the angle between the prime meridian passing through the south, and the projection of the sun on the equatorial plane (Figure 4). It measures the sun's path in the sky [12]. It is counted positively in the morning and negatively at the afternoon [13]. It increases by five degrees per hour.

H is given by the following expression [6]:

$$H = 15^{\circ}(RTS - 12) \quad (2)$$

RTS is counted from 0 to 24 h. It is calculated by the following relation:

$$RTS = T_{legal} + ET - \frac{L - L_{ref}}{15} - C \quad (3)$$

where:

- *ET* is the correction of the equation of time, due to the variation in the speed of the earth on its path around the sun. This correction varies between 14 minutes minimum and 17 minutes maximum [9]. As a function of the day number *n*, counted from 1 to 365, *ET* is expressed by the following expression [14]:

$$ET = -0.0002 + 0.47497 \cos(x) - 7.3509 \sin(x) - 3.2265 \cos(2x) - 9.3912 \sin(2x) - 0.0903 \cos(3x) - 0.3361 \sin(3x) \quad (4)$$

with:

$$x = 360n / 366 \quad (5)$$

- *T_{legal}*: Legal Time is the time that is commonly used. It is shifted by a integer number of hours compared to the origin time (Meridian 0).
- *L-L_{ref}*: Longitude difference between a considered place and the longitude reference in standard time.
- *C*: Time difference that is the difference between the standard time and the calendar time zone where it is located.

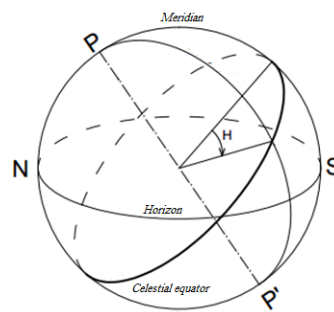


Figure 4. Hours Celestial Coordinate

3.1.2.2. Horizontal Celestial Coordinates

This coordinate system (Figure 5) has a reference the horizontal plane. The sun is located by two components: its altitude angle *h* and its azimuth *a*.

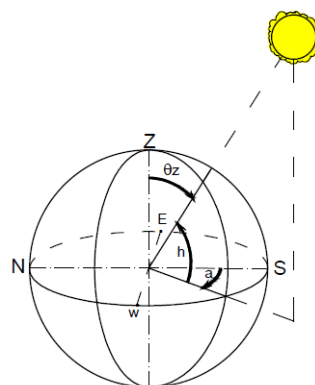


Figure 5. Horizontal Celestial Coordinates

a) Sun Altitude h

This is the angle between the apparent direction of the sun and its projection on the horizontal plane [12], [9], h may vary during the day from 0° (sun on the horizon) to 90° (midday sun). h is a function of the declination δ , the latitude φ and the hour angle H according to the following relation [6]:

$$\sin(h) = \cos(\delta)\cos(\varphi)\cos(H) + \sin(\varphi)\sin(\delta) \quad (6)$$

b) Sun Azimuth a_s

It is the angle between the projection of the sun direction on the horizontal plane and north or south direction. It is comprised between -180° and $+180^\circ$. According to δ declination, the hour angle H , the height h and the longitude L , the azimuth is calculated by the following equations [13]:

The angle between the direction of the sun with the vertical is called zenith angle θ_z . It varies from 0° to 90° according to the following relation:

$$\theta_z = 90^\circ - h \quad (8)$$

According to declination δ , the latitude φ and height h , the zenith angle θ_z , it can be calculated by:

$$\cos(\theta_z) = \cos(\delta)\cos(\varphi)\cos(h) + \sin(\varphi)\sin(\delta) \quad (9)$$

3.1.1. Plane Orientation

An arbitrary orientation plane as illustrated in Figure 6 can be located by two angles h_p and a_p with:
 h_p : The height of the plane is the angle between the normal \vec{n} to the plane and its projection on the horizontal plane.

a_p : Plane azimuth that represents the angle between the projection of the normal \vec{n} on the horizontal plane and south direction [12].

The inclination of the plane relatively to the horizontal plane is designated by β angle. This latter varies between 0° and 90° . This angle is given by the following formula [12]:

$$\beta = 90^\circ - h_p \quad (10)$$

The angle between the direction of the sun and the normal \vec{n} to the plane is called incidence angle θ_i , which is determined by the following equation [15]:

$$\begin{aligned} \cos(\theta_i) = & \sin(\delta)\sin(\varphi)\cos(\beta) - \sin(\delta)\cos(\varphi)\sin(\beta)\cos(a_p) \\ & + \cos(\delta)\cos(\varphi)\cos(\beta)\cos(H) + \cos(\delta)\sin(\varphi)\sin(\beta)\cos(a_p)\cos(H) \\ & + \cos(\delta)\sin(\beta)\sin(a_p)\sin(H) \end{aligned} \quad (11)$$

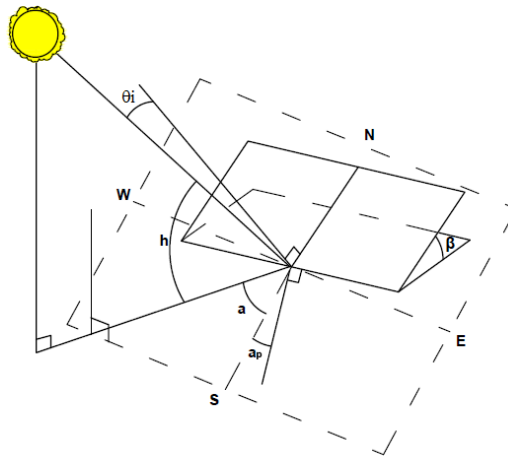


Figure 6. Plane Orientation

3.2. Modeling of the Incident Solar Radiation on a Horizontal Plane

The global solar radiation G on a horizontal plane is the sum of two components: the direct solar radiation and diffuse solar radiation [16] (Figure 7).

$$G = G_{dir} + G_{diff} \quad (12)$$

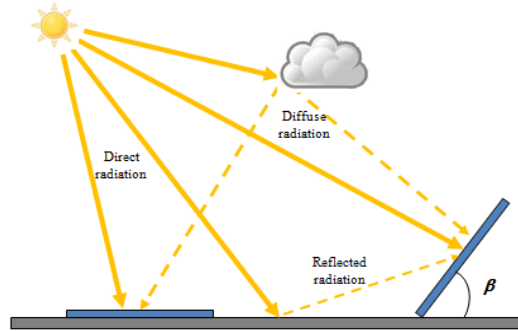


Figure 7. Global Solar Radiation Received on a Horizontal Plane and on a Tilted One

- The direct radiation G_{dir} is a quasi-parallel solar irradiance, coming from the solar disc intercepted most of the time, by a normal surface to the direction of the sun. It is measured by a Pyrheliometer.
- The diffuse radiation G_{diff} is a solar radiation received by any surface and coming from the whole hemisphere seen from the surface except the solar disk. It is measured using a pyranometer protected from direct solar radiation by a screen.

The direct solar radiation on a horizontal plane is given by the following equation [13]:

$$G_{dir} = I^* \sin(h) \quad (13)$$

where I^* is a direct sun light incident on the Earth surface of, it is expressed by the following formula [17]:

$$I^* = (I_0)_{ext} \exp\left[-\frac{m_h T_L}{0.9m_h + 9.4}\right] \quad (14)$$

with:

- $(I_0)_{ext} = 1366 \text{ W/m}^2$: The constant corresponding to the extraterrestrial solar radiation;
- m_h : The atmospheric optical distance, called air mass (m). This latter is the ratio of the traveled distance in the atmosphere by a ray coming from the sun to the vertical thickness of the atmosphere measured at sea level [9]. For Z altitude, atmospheric mass expressed by using the following equation applied by *Kasten* in 1959 [17]:

$$m_h = \frac{1 - 0.1Z}{\sin(h) + 0.15(h + 3.885)^{-1.253}} \quad (15)$$

- T_L : Is the *Linke* turbidity factor. It gives an evaluation of the atmospheric extinction by gaseous molecules and aerosols. Its average value is given by the following relation [9]:

$$T_L = 2.5 + 16\beta_A + 0.5 \ln(w) \quad (16)$$

where:

- β_A is the Angstrom coefficient that characterizes the clarity of the sky. This coefficient is determined by the number of aerosols enclosed in an air mass unit vertically at the measurement place. The Table 1 gives some values;
- w is the height of condensable water (in cm). It corresponds to the respective thickness of water that would be obtained by the condensation of any water vapor contained in a hypothetical cylinder with the axis parallel to the solar rays. The table 1 gives some values.

Table 1. Values of the Angstrom Coefficient and the Condensable Water Height for Three States

Atmospheric		
Case	β_A	w (cm)
The clear sky	0.05	1
Sky moderately cloudy	0.1	2
Sky very cloudy	0.2	5

The diffuse radiation is given by the following equation [14]:

$$G_{diff} = \frac{(I_0)_{ext}}{25} \sqrt{\sin(h)} \left[T_L - 0.5 - \sqrt{\sin(h)} \right] \quad (17)$$

3.3. Modeling of the Incident Solar Radiation on a Tilted Plane

In order to better quantify the amount of solar radiation received by the inclined PV modules, some kind of correction should be made regarding the solar radiation on a horizontal surface. This task will be necessarily for estimating the incident radiation received by an inclined surface.

The general shape of the overall radiation received on a β inclined plane is given by:

$$G_{\beta} = G_{dir,\beta} + G_{ref,\beta} + G_{diff,\beta} \quad (18)$$

The incident direct solar radiation on an inclined surface $G_{dir,\beta}$ can be estimated by multiplying its value on a horizontal surface G_{dir} by a geometric factor R_b which depends on the zenith angle θ_z and the incidence angle θ_i which depends on β according to the equation (11). Thus, the following relation gives $G_{dir,\beta}$:

$$G_{dir,\beta} = G_{dir} R_b = G_{dir} \frac{\cos(\theta_i)}{\cos(\theta_z)} \quad (19)$$

The solar radiation reflected by the ground and received by a tilted plane can be estimated by multiplying the total radiation on a horizontal surface G by the ground reflectance ρ called albedo, and the visibility factor between the surface and the ground, as shown by the equation below [18]:

$$G_{ref,\beta} = \frac{1}{2} \rho G (1 - \cos \beta) \quad (20)$$

The diffuse solar radiation on the inclined plane, can be evaluated according to the model *Klucher* [19] given by the following equation:

$$G_{diff,\beta} = G_{dir} \left[0.5 \left(1 + \cos\left(\frac{\beta}{2}\right) \right) \right] \left[1 + F \sin^3\left(\frac{\beta}{2}\right) \right] \left[1 + \cos^2(\theta_i) \sin^3(\theta_z) \right] \quad (21)$$

with:

$$F = 1 - \left(\frac{G_{diff}}{G} \right)^2 \quad (22)$$

4. MODELING OF PVG

In this section, we present three models for modeling the electrical characteristics of our PVG.

4.1. Simplified Model with a Single Diode with R_s

4.1.1. Presentation of R_s Model

This model is a simplified model based on the equivalent circuit with a diode given in Figure 8. The characterizing equation of this model is as follows [21-22]:

$$I_{pv} = I_{ph} - I_0 \left[\exp \left(\frac{q(V_{pv} + R_s I)}{n_s a K T_{cell}} \right) - 1 \right] \quad (23)$$

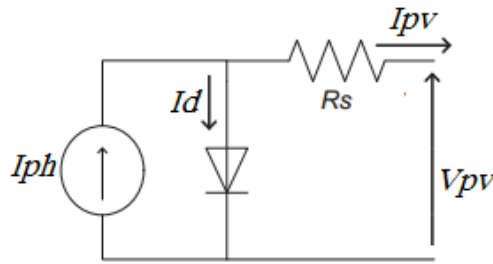


Figure 8. R_s Model

In the following, we assume the approximation $I_{ph} = I_{sc}$ where I_{sc} is function of the temperature of the cells T_{cell} and the radiation G_β , this current is expressed by:

$$I_{sc} = I_{sc,ref} \left[1 + \alpha_0 (\Delta T) \right] \frac{G_\beta}{G_{\beta,ref}} \quad (24)$$

ΔT is the temperature difference, which is calculated by the equation:

$$\Delta T = T_{cell} - T_{cell,ref} \quad (25)$$

With $T_{cell,ref} = 25^\circ\text{C}$ and T_{cell} varies depending on the radiation and the ambient temperature T_a according to the following linear relation:

$$T_{cell} = T_a + \frac{(NOCT - 20)G_\beta}{800} \quad (26)$$

where $NOCT$ is the Nominal Operating Cell Temperature.

For the reference temperature $T_{cell,ref}$, the reference's reverse saturation current $I_{0,ref}$ can be calculated from equation (23), where $I_{pv} = 0$; corresponding to the open circuit case $V_{pv} = V_{oc,ref}$. This current $I_{0,ref}$ is expressed by:

$$I_{0,ref} = \frac{I_{sc,ref}}{\exp \left(\frac{qV_{oc,ref}}{n_s a K T_{cell,ref}} \right) - 1} \quad (27)$$

The dependence of the reverse saturation current of the diode I_0 , for any T_{cell} temperature can be expressed by the following equation [23]:

$$I_0 = I_{0,ref} \left(\frac{T_{cell,ref}}{T_{cell}} \right)^{\frac{3}{a}} \exp \left[\frac{qE_g}{aK} \left(\frac{1}{T_{cell,ref}} - \frac{1}{T_{cell}} \right) \right] \quad (28)$$

Where E_g is the Gap that means the energy of the band gap of the semiconductor, such as $E_g = 1.2$ eV for poly-crystalline silicon at 25°C .

4.1.2. R_s model Parameter Extraction

Figure 9 presents the simplified iterative algorithm of R_s model.

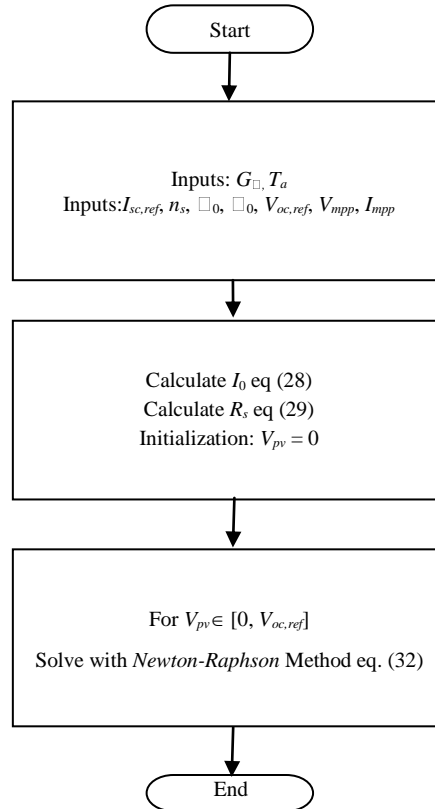


Figure 9. Algorithm Resolving the R_s Model

By neglecting the term "-1" added to the exponential equation (23), the value of R_s can be obtained by the following equation:

$$R_s = - \left. \frac{dV_{pv}}{dI_{pv}} \right|_{V_{pv} = V_{oc}} - \frac{1}{X_v} \quad (29)$$

with:

$$X_v = q \frac{I_{sc}}{aKT_{cell}} \quad (30)$$

The equation (29) term $(-dV_{pv}/dI_{pv})$ can be determined experimentally from the I_{pv} - V_{pv} characteristic given by the manufacturer.

To solve the equation (23), it can be written in the following form:

$$I_{pv} - I_{ph} + I_0 \left[\exp \left(\frac{q(V_{pv} + R_s I)}{n_s a K T_{cell}} \right) - 1 \right] = 0 \quad (31)$$

So that we have:

$$f(I) = I_{pv} - I_{ph} + I_0 \left[\exp \left(\frac{q(V_{pv} + R_s I)}{n_s a K T_{cell}} \right) - 1 \right] = 0 \quad (32)$$

The *Newton-Raphson* method is used for determining the solution of this equation (23), by applying the following iterative relation:

$$I_{pv,k+1} = I_{pv} - \frac{f(I_{pv,k})}{f'(I_{pv,k})} \quad (33)$$

with:

$f(I_{pv})$: Function to solve and $f'(I_{pv})$ its derivative;
 $I_{pv,k}$: k^{th} iteration of the current;
 $I_{pv,k+1}$: $(k+1)^{\text{th}}$ iteration of the current.

4.2. Model with One Diode with R_s and R_p

4.2.1. Presentation of the R_s - R_p Model

Some authors [24] have developed this model, shown in Figure 10. It's also based on the equivalent circuit with a diode in addition to the series resistor. This model takes account of the parallel resistor effect, called shunt resistor (R_p). This model ensures that the maximum power of the model corresponds to the real maximum power of the PV module. In the case of this model, the current I_{pv} is given by the equation below [25-26].

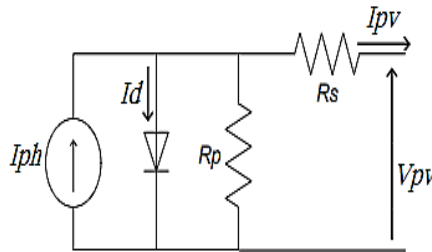


Figure 10. R_s - R_p Model

$$I_{pv} = I_{ph} - I_d - I_{sh} \quad (34)$$

The photo-current is linearly dependent on solar radiation but also influenced by the temperature, according to the following relation:

$$I_{ph} = (I_{ph,ref} + \alpha_0 \Delta T) \frac{G_\beta}{G_{\beta,ref}} \quad (35)$$

In the standard test conditions or nominal conditions ($G = 1000 \text{ W/m}^2$ and $T = 298 \text{ K}$), the expression of $I_{ph,ref}$ is given by :

$$I_{ph,ref} = \left(1 + \frac{R_s}{R_p}\right) I_{sc,ref} \quad (36)$$

Therefore, the final expression of the photocurrent I_{ph} is given by the following equation:

$$I_{ph} = \left(\left(1 + \frac{R_s}{R_p} \right) I_{sc,ref} + \alpha_0 \Delta T \right) \frac{G_\beta}{G_{\beta,ref}} \quad (37)$$

By application of the meshes law, the I_{sh} current in the shunt resistor is expressed by [27]:

$$I_{sh} = \frac{V_{pv} + R_s I_{pv}}{R_p} \quad (38)$$

The diode current I_d is given by:

$$I_d = I_0 \left[\exp \left(\frac{V_{pv} + R_s I_{pv}}{V_t a} \right) - 1 \right] \quad (39)$$

with:

$$V_t = \frac{n_s a K T_{cell}}{q} \quad (40)$$

By replacing T_{cell} in equation (40) by $T_{cell,ref}$, we obtain the thermal voltage $V_{t,ref}$ at the reference temperature $T_{cell,ref}$:

$$V_{t,ref} = \frac{n_s a K T_{cell,ref}}{q} \quad (41)$$

The reverse saturation current of diode I_0 given by (28) can be calculated by the following equation:

$$I_0 = \frac{I_{sc,ref} + \alpha_0 \Delta T}{\exp \left(\frac{V_{oc,ref} + \beta_0 \Delta T}{a V_t} \right) - 1} \quad (42)$$

Finally, the current I_{pv} of the equation (34) becomes:

$$I_{pv} = I_{ph} - I_0 \left[\exp \left(\frac{V_{pv} + R_s I_{pv}}{V_t a} \right) - 1 \right] - \frac{V_{pv} + R_s I_{pv}}{R_p} \quad (43)$$

4.2.2. R_s - R_p Model Parameter Extraction

Some authors [24], suggest a method allowing the determination of the two R_s and R_p unknown parameters of the (43) equation. Their method is based on the fact that a unique pair (R_s , R_p) exists that guaranties the equality between the maximum power $P_{max,c}$ given the manufacturer and the maximum power $P_{max,s}$ calculated using the model.

The relation between R_p and R_s can be determined by satisfying the condition of $P_{max,c} = P_{max,s}$ and solving the resulting equation as follows:

$$P_{max,s} = V_{mpp} \left\{ \begin{array}{l} I_{ph} - I_0 \left[\exp \left(\frac{q}{K T_{cell}} \frac{V_{mpp} + R_s I_{mpp}}{a n_s} \right) - 1 \right] \\ - \frac{V_{mpp} + R_s I_{mpp}}{R_p} \end{array} \right\} \quad (44)$$

$$= P_{max,c}$$

From equation (44), the value of R_p is determined, as indicated by the following equation:

$$R_p = \frac{V_{mpp}(V_{mpp} + I_{mpp}R_s)}{\left\{ V_{mpp}I_{ph} - V_{mpp}I_0 \exp\left[\frac{(V_{mpp} + I_{mpp}R_s) - q}{n_s a} \frac{q}{KT} \right] + V_{mpp}I_0 - P_{max,c} \right\}} \quad (45)$$

This latter equation shows that for each value of R_s corresponds a value of R_p such that the characteristic $I_{pv}-V_{pv}$ passes by the point (V_{mpp}, I_{mpp}) . In order that the iterative process starts, the initial estimation of R_s and R_p is necessarily. The R_p initial value $R_{p,min}$ can be calculated by the use of the equation:

$$R_{p,min} = \frac{V_{mp}}{I_{sc,ref} - I_{mp}} - \frac{V_{oc,ref} - V_{mp}}{I_{mp}} \quad (46)$$

Simplified iterative algorithm of R_s-R_p model is presented in Figure 11, with x_1, x_2, x_3, x_4 and x_5 are respectively the equations 42, 46, 37, 45 and 35.

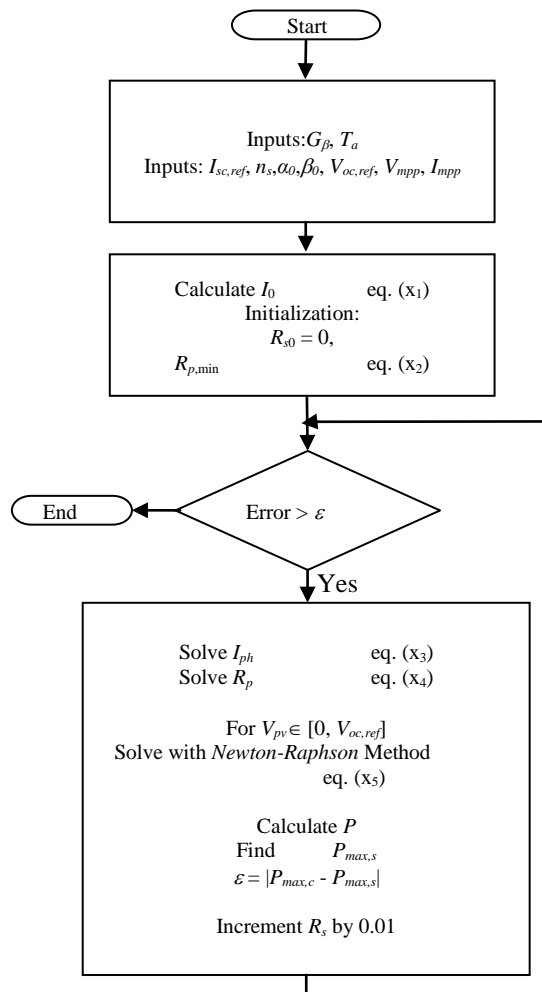


Figure 11. Algorithm Resolving the R_s-R_p Model

4.3. Model Two Diode

4.3.1 Presentation of Model Two Diode

Other authors [28] presented this model. It's a model that was simplified and uses only four parameters comparatively to six or more in other models of two diodes. It's founded on the equivalent circuit

given by the Figure 12. We realize this circuit by connecting in parallel two diodes. The saturation current of the two diodes are I_{01} and I_{02} and the ideality factors are a_1 and a_2 .

The following equation describes the output current of the PV generator:

$$I_{pv} = I_{ph} - I_{d1} - I_{d2} - \left(\frac{V_{pv} + R_s I_{pv}}{R_p} \right) \quad (47)$$

with I_{d1} and I_{d2} the respective currents of the diodes 1 and 2. They are expressed by the equations (48) and (49):

$$I_{d1} = I_{01} \left[\exp \left(\frac{V_{pv} + R_s I_{pv}}{a_1 V_{T1}} \right) - 1 \right] \quad (48)$$

$$I_{d2} = I_{02} \left[\exp \left(\frac{V_{pv} + R_s I_{pv}}{a_2 V_{T2}} \right) - 1 \right] \quad (49)$$

Authors who developed this model [28], assumes that the saturation currents I_{01} and I_{02} are equal (equation 50):

$$I_0 = I_{01} = I_{02} = \frac{(I_{sc,ref} + \alpha_0 \Delta T)}{\exp \left[\frac{(V_{oc,ref} + \beta_0 \Delta T)}{((a_1 + a_2)/p)V_t} \right] - 1} \quad (50)$$

According to the Shockley diffusion theory, a_1 must be equal to 1 [28-29]. A value of a_2 greater than or equal to 1.2 gives a better match between the proposed model and practice characteristics $I_{pv}-V_{pv}$.

The value of the variable p can be chosen greater or equal to 2.2 since $a_1 = 1$ and $(a_1 + a_2)/p = 1$ [28].

The photo-current I_{ph} can be calculated, as a function of the temperature of the cells T_{cell} and the radiation G_β , as previously for the case of model R_s-R_p .

$$I_{ph} = (I_{ph,ref} + \alpha_0 \Delta T) \frac{G_\beta}{G_{\beta,ref}} \quad (51)$$

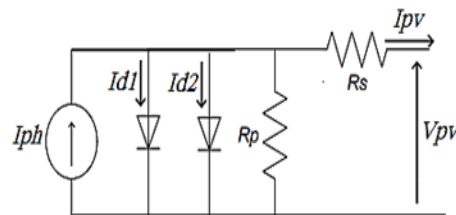


Figure 12. Two Diodes Model

4.3.2. Parameter Extraction of Model Two Diode

The value of the resistor R_p is determined, as in the case of the model R_p-R_s , satisfying the condition of equality between the power given by the manufacturer $P_{max,c}$, and the maximum power $P_{max,s}$ calculated by the model.

$$R_p = \frac{V_{mpp} (V_{mpp} + R_s I_{mpp})}{\left[V_{mpp} (I_{ph} - I_{d1} - I_{d2}) - P_{max,c} \right]} \quad (52)$$

The initial value for the resistor R_s is $R_{s0} = 0$ however the initial value of the resistor R_{p0} is estimated by:

$$R_p = \frac{V_{mpp} (V_{mpp} + R_s I_{mpp})}{V_{mpp} (I_{ph} - I_{d1} - I_{d2}) - P_{max,c}} \tag{53}$$

The simplified iterative algorithm of the two diodes model is shown in Figure 11, with x_1, x_2, x_3, x_4 and x_5 are respectively the equations 50, 53, 51, 52 and 47.

5. RESULTS AND DISCUSSION

5.1. Estimation of the Incident Solar Radiation

In order to validate the used model to predict the real global solar radiation received by horizontal surface, we conducted the measurements on a sample recorded by the weather station installed in the site under study. Those measurements cover a long period stretching from 2009 to 2013. The Figures 13 to 16 compare the solar radiation given by the station with the one delivered by our model developed under Matlab for 4 days: November 15th, 2013, March 12th, 2012, July 01st, 2011 and September 11th, 2009.

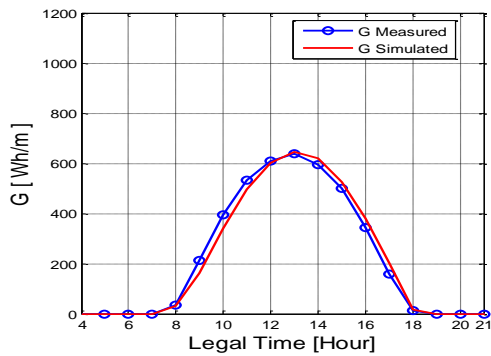


Figure 13. Global Solar Radiation Received on a Horizontal Surface on November 15th, 2013.

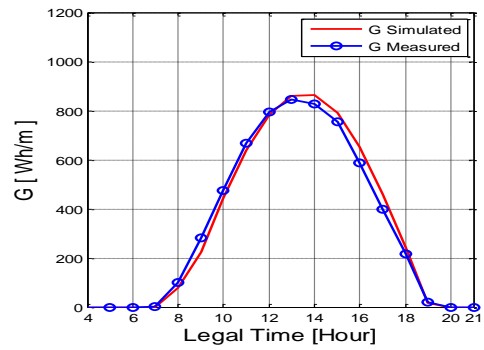


Figure 14. Global Solar Radiation Received on a Horizontal Surface on March 12th, 2012

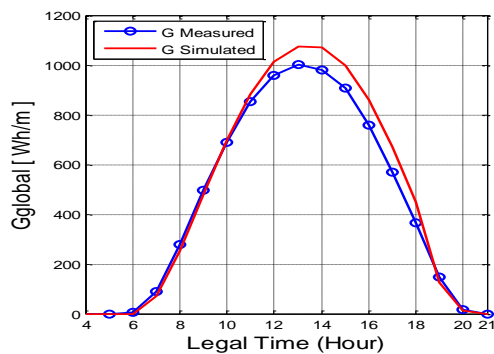


Figure 15. Global Solar Radiation Received on a Horizontal Surface on July 01st 2011

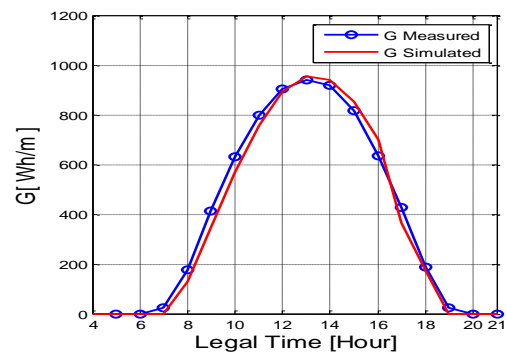


Figure 16. Global Solar Radiation Received on a Horizontal Surface on September 11th, 2009

In order to judge the reliability of the proposed model at our site and in order to determine the error of the incident radiation, we calculate the instantaneous relative error by the following equation:

$$Err = \frac{G_{measured} - G_{calculated}}{G_{measured}} \tag{54}$$

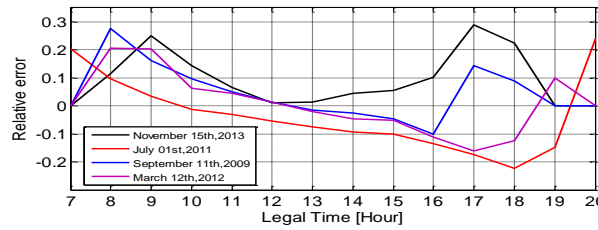


Figure 17. Relative Error of the Global Solar Radiation Received on a Horizontal Surface for the Selected Four Days

The error's values for the four days of the selected sample are showing in Figure 17. These values show that the instantaneous relative error does not exceed 10 % from 10:00 AM to 4:00 PM, and the maximum of this error is 27 % for November 15th 2013, 06:00 PM. This confirms the validity of our model.

For inclined surfaces of angles $\beta = 15^\circ, 30^\circ, 45^\circ$ and 60° , we have represented in figure 18 the global solar radiation G_β received on these surfaces. We observe an increase of solar radiation received by the inclined surfaces compared to the horizontal ones, which leads to the increasing of the power produced by the PVG.

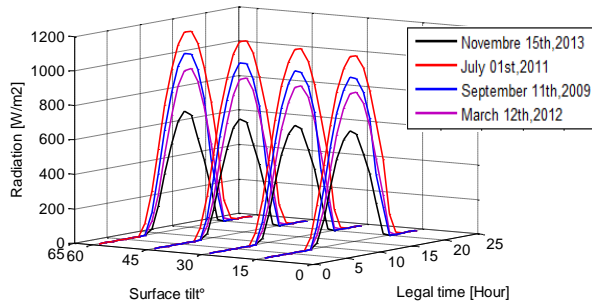


Figure 18. Global Solar Radiation for Different Inclinations at the 4 Selected Days

5.2. Extracting the Electrical Parameters of the PVG

The PVG, which is the object of our characterization, is of type BP Solar MSX-64. Its electrical characteristics are provided in Table 2 [30].

Table 2. Electrical Characteristics of the PV Panel MSX-64

Maximum power $P_{max,c}$	64 W
Voltage at maximum power V_{mpp}	17.5 V
Current at maximum power I_{mpp}	3.66 A
Short-circuit current $I_{sc,ref}$	4 A
Open-circuit voltage $V_{oc,ref}$	21.3 V
Temperature coefficient β_0 of V_{oc}	$-(80 \pm 10)$ mV/ $^\circ$ C
Temperature coefficient α_0 of I_{sc}	(0.065 ± 0.015) %/ $^\circ$ C
Temperature coefficient γ_0 of power	$-(0.5 \pm 0.05)$ %/ $^\circ$ C
NOCT	47 ± 2 $^\circ$ C

For the three models used to model and characterize our PVG, we have represented in the same Figures 19 to 21, the output characteristics $I_{pv}-V_{pv}$ and simulated power $P_{pv}-V_{pv}$ as well as those given by the

manufacturer, under radiation $G_{\beta} = 1000 \text{ W/m}^2$ and temperatures of 25 °C, 50 °C and 75 °C.

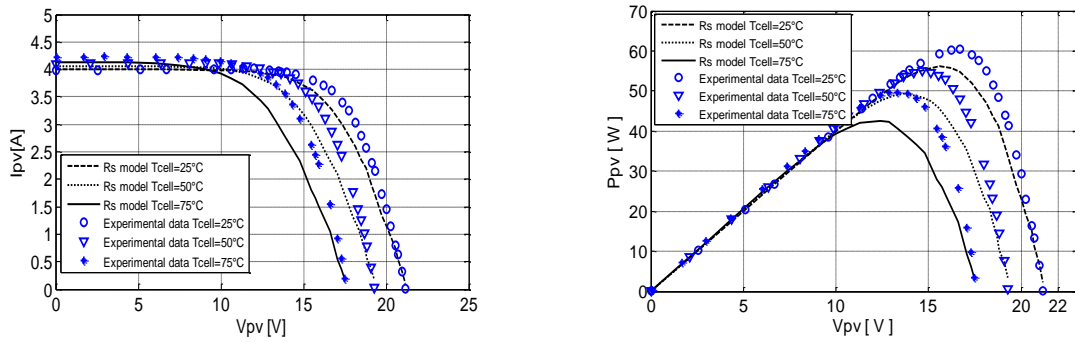


Figure 19. Extracted Characteristics I_{pv} - V_{pv} and P_{pv} - V_{pv} from R_s Model (for $G_{\beta} = 1000 \text{ W/m}^2$ and $T_{cell} = 25 \text{ }^{\circ}\text{C}$, 50°C and $75 \text{ }^{\circ}\text{C}$)

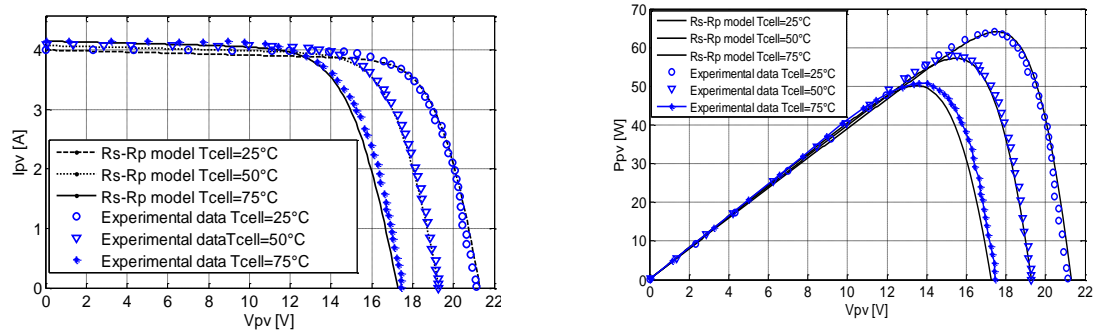


Figure 20. Extracted characteristics I_{pv} - V_{pv} and P_{pv} - V_{pv} from R_s - R_p model (for $G_{\beta} = 1000 \text{ W/m}^2$ and $T_{cell} = 25, 50$ and $75 \text{ }^{\circ}\text{C}$)

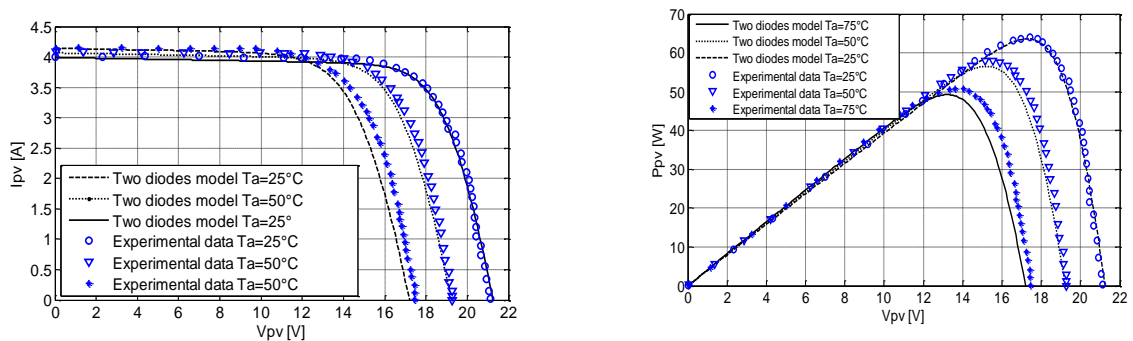


Figure 21. Extracted characteristics I_{pv} - V_{pv} and P_{pv} - V_{pv} from two diodes model (for $G_{\beta} = 1000 \text{ W/m}^2$ and $T_{cell} = 25, 50$ and $75 \text{ }^{\circ}\text{C}$)

Table 3. Extracted Parameters for the three models

Parameters	R_s Model	R_s - R_p Model	Model 2 diodes
R_s (Ω)	0.32	0.28	0.26
R_p (Ω)	-	115.70	123.45
$P_{max,s}$ (W)	56.26	64.05	64.05
$P_{max,c}$ (W)	64.05	64.05	64.05
Erreur (W)	7.79	0.0001	0
I_0 (A)	$7.51 \cdot 10^{-7}$	$3.813810 \cdot 10^{-10}$	$3.988721 \cdot 10^{-10}$

As a result of the comparison of the various figures 19 to 21, we observe that, for both models, R_s-R_p and two diodes, the simulated output characteristics reproduce quite faithfully the experimental data of the manufacturer contrarily to R_s model.

After treatment of the three proposed models, we summarize in Table 3, the results for the electrical parameters extracted from the modeled PVG.

In order to confirm the previous observations and to estimate the precision of the extracted parameters from the suggested models that represented the $I_{pv}-V_{pv}$ characteristics, we calculated the absolute error Era that represents the difference between the I_{pv} measured currents by the manufacturer and those calculated by modeling and simulated. The following relation expresses the absolute difference Era :

$$Era = |I_{pv \text{ measured}} - I_{pv \text{ calculated}}| \quad (55)$$

Thus, the evaluated errors are shown in Figure 22 in the case of $I_{pv}-V_{pv}$ characteristics in the weather conditions $G_\beta = 1000 \text{ W/m}^2$ and $T_{cell} = 25 \text{ }^\circ\text{C}$, $50 \text{ }^\circ\text{C}$ and $75 \text{ }^\circ\text{C}$.

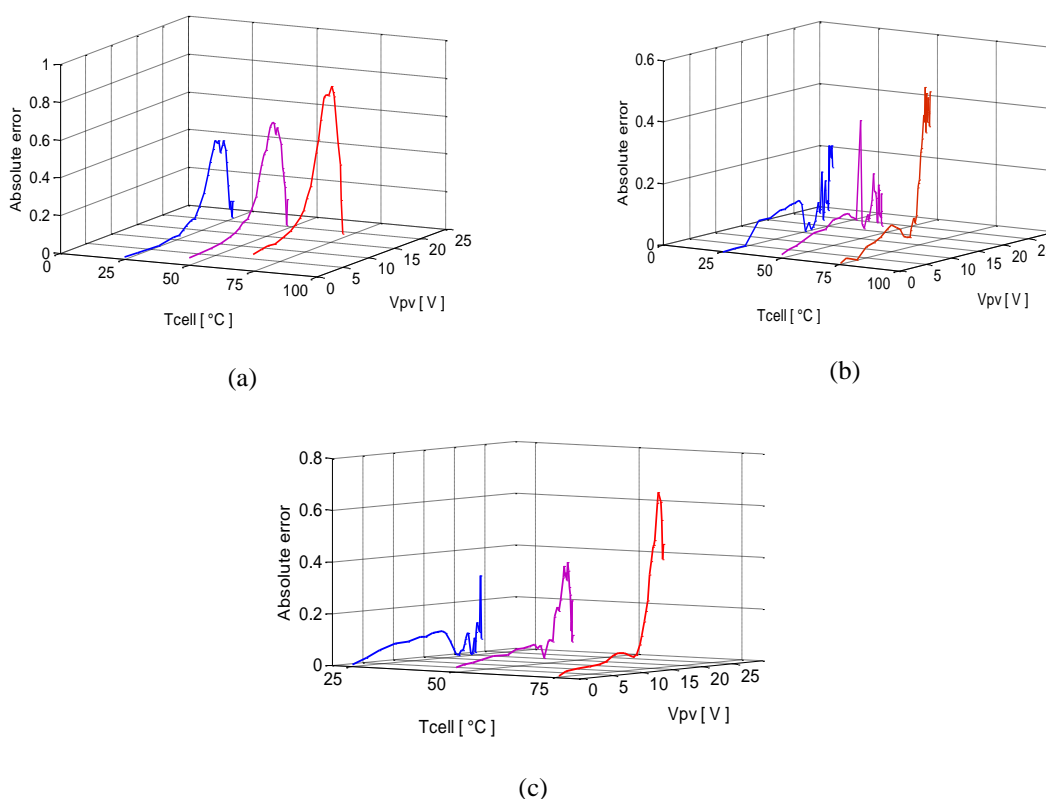


Figure 22. Absolute Errors Evaluating the three models: R_s (a), R_s-R_p (b) and the 2diodes (c)

Basing on the Figure 22, we can notice that for both models R_s-R_p and a two diode model, the absolute deviations Era are quite low. This is in agreement with the results that Villalva and al found in [24] during the modelling and the simulation of two modules PV (KC200GT and MSX60) by the application of the R_s-R_p model and with the results that Khassif and al found in [28] to model and simulate the electric behavior of six PV modules (MSX-60, KG200GT, S36, SG150-PC, SP 70 and ST40). For that reason, those the two models will be selected to describe the output characteristic of the PV module under test; BP Solar MSX-64.

5.3. Prediction of the Power Produced by PVG

The figure 23 shows the output characteristic as well as the estimated electrical power produced by the BP Solar MSX-64, for different inclinations, November 15th 2013 at 2:00 PM.

Finally, the adopted approach allows us to predict $I_{pv}-V_{pv}$ and $P_{pv}-V_{pv}$ characteristics of a PV module for any orientation and any location.

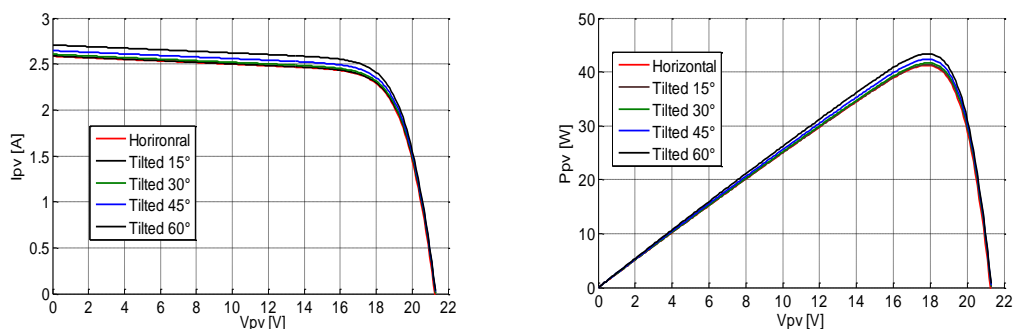


Figure 23. Estimated characteristics V_{pv} - I_{pv} and P_{pv} - V_{pv} at November 15th 2013 at 02:00 PM

6. CONCLUSION AND PERSPECTIVES

The work presented in this paper allowed us to predict the output current-voltage and the power-voltage characteristics of a photovoltaic generator installed in a selected location, and consequently estimating the daily, monthly and yearly production of electricity, in other words, the determination of the photovoltaic system performance.

The measurements collected by the weather station installed in our laboratory, has allowed us to validate the selected model for the prediction and estimation of the incident solar radiation on the horizontal surfaces.

Modeling and characterization the photovoltaic generator allowed us to confirm that the R_s - R_p model and the model with two diodes provide a good agreement between the manufacturer experimental data and the simulated data.

The prospects of our work are, firstly to connect the modeled PVG to a storage element through an adaptation floor provided with a search function of a maximum power point tracking (MPPT) to extract the maximum of power. Secondly, we aim the insertion of this PV conversion chain in a hybrid system of renewable energy.

REFERENCES

- [1] A. Orioli, A. Di Gangi. A procedure to calculate the five-parameter model of crystalline silicon photovoltaic modules on the basis of the tabular performance data. *Applied Energy*. 2013; 102: 1160-1177.
- [2] L. Stoyanov. Etude de différentes structures de systèmes hybrides à sources d'énergie renouvelables. Thèse de doctorat. Université de Corse Pasquale Paoli. 2011.
- [3] A.D. Jones and C.P. Underwood. A Modeling Method for Building-integrated Photovoltaic Power Supply. *Building Services Engineering Research and Technology*. 2002; 23(3): 167-177.
- [4] S. Farhat, R. Alaoui, A. Kahaji, L. Bouhouch. MPPT Efficiency test by neural networks and P&O algorithm, *International Review of Electrical Engineering (IREE)*. 2013; 8(5): 1548-1555.
- [5] S. Farhat, R. Alaoui, A. Kahaji, L. Bouhouch. P&O and Incremental Conductance MPPT Implementation. *International Review of Electrical Engineering (IREE)*. 2015; 10(1): 116-122.
- [6] R. Chenni, E. Matagne, M. Khennane. Study of solar radiation in view of photovoltaic systems optimization. *Smart Grid and Renewable Energy*. 2011; 2: 367-374.
- [7] T. Maatallah, S. El Alimi, S. Ben Nassallah. Performance modeling and investigation of fixed, single and dual-axis tracking photovoltaic panel in Monastir city, Tunisia. *Renewable and Sustainable Energy Reviews*. 2011; 15(8): 4053-4066.
- [8] http://fr.wikidia.org/wiki/Mouvement_apparent_du_Soleil
- [9] M.A. Camara, Modélisation du stockage de l'énergie photovoltaïque par super-condensateurs, Thèse de doctorat, Université Paris-Est Creteil. 2011.
- [10] G. Notton, C. Poli, S. Vasileva, M.L. Nivet, J.L. Canaletti, C. Cristofari. Estimation of hourly global solar irradiation on tilted planes from horizontal one using artificial neural networks. *Energy*. 2012; 39: 166-179.
- [11] R. PonVengatesh, S. Edward Rajan. Investigation of cloudless radiation with PV module employing Matlab-Simulink. *Solar Energy*. 2011; 85: 1727-1734.
- [12] Sidi Mohammed Elamin Bekkouche. Modélisation thermique de quelques dispositifs solaire. Thèse de doctorat, Université Abou-Bakr Belkaid Tlemcen. 2009.
- [13] A. M'Raoui, S. Mouhous, A. Malek, B. Benyoucef. Etude statistique du rayonnement solaire à Alger. *Revue des Energies Renouvelables*. 2011; 14(4): 637-648.

- [14] B. Ould Bilal, V. Sambou, C.M.F. Kebe, M. Ndong, P.A Ndiaye. Etude et modélisation du potentiel du site de Nouakchott et de Dakar. *Journal des Sciences*. 2007; 7(4): 57-66.
- [15] E.D. Mehleri, P.L. Zervas, H. Sarimveis, J.A. Palyvos, N.C. Markotos. Determination of the optimal tilt angle and orientation for solar photovoltaic arrays. *Renewable Energy*. 2010; 35: 2468-2475.
- [16] Andrea Padovan, Davide Del Col. Measurement and modeling of solar irradiance components on horizontal and tilted planes. *Solar Energy*. 2010; 84: 2068-2084.
- [17] P. Henri Communay. Héliothermique: le gisement solaire méthodes et calculs. Groupe de recherche et d'édition. 2002.
- [18] M. Iqbal, An introduction to solar radiation, Academic de press, Canada, 1983, ISBN: 0-12-373752-4, 1983.
- [19] T.M. Klucher. Evaluation of models to predict insolation on tilted surfaces, *Solar Energy*. 1979; 23(2): 111-114.
- [20] Djamilia Rekioua, Ernest Matagne. Optimization of Photovoltaic Power Systems, Book, Springer, ISBN 978-1-4471-2348-4. 2012.
- [21] Fu Qiang, Tong Nan. A strategy research on MPPT technique in photovoltaic power generation system. *TELEKOMINIKASIA*. 11(12): 7627-7633.
- [22] Mohamed Louzazni, EL Hassan Aroudan, Hanane Yatimi. Modeling and simulation of solar power source for a clean energy without pollution. *International Journal of Electrical and Computer Engineering (IJECE)*. 2013; 3(4): 568-576.
- [23] Francisco M. Gonzalez-Longatt. *Model of photovoltaic Module in Matlab*, 2DoCongresoIbero Americano de Estudiantes de Ingenieria Electrica, Electronicay Computacion. CIBELEC. 2005.
- [24] M. Gradella Villalva, J. Rafael Gazoli and E. Ruppert Filho. Comprehensive Approach to Modelling and Simulation of Photovoltaic Arrays. *IEEE Transactions on Power Electronics*. 2009; 24(5): 1198-1208.
- [25] Mohammed Yaichi, Mohammed Karim Fella, Abdelkrim Mammeri. A Neural Network Based MPPT Technique controller for pumping system. *International Journal of Power Electronics and Drive System (IJPEDS)*. 2014; 4(2): 241-255.
- [26] Sangita R. Nandurkar, Mini Rajeev. Design of photovoltaic array with MPPT control techniques. *International Journal of Applied Power Engineering (IJAPE)*. 2014; 3(1): 41-50.
- [27] Sobhan Dorahaki. A survey on maximum power point tracking methods in photovoltaic power systems. *Bulletin of Electrical Engineering and Informatics*. 2015; 4(3):169-175.
- [28] K.Ishaque, Zainal Salam, Hamed Taheri. Simple fast and accurate two-diode model for photovoltaic modules. *Solar Energy Materials & Solar cells*. 2011; 95: 586-594.
- [29] C. Sah, Fundamentals of solid-state electronics, World Scientific publishing Co. Pte, Library of Congress Cataloging-in-Publication Data, ISBN 9810206372, 1991.
- [30] <https://www.smud.org/en/about-smud/environment/renewable-energy/documents/solar-regatta-photovoltaic-specs.pdf>

BIOGRAPHIES OF AUTHORS



Mustapha Elyaqouti was born in Agadir, Morocco, in 1984. He received the technical University degree (DUT) in Electrical Engineering from the High School of Technologies of Agadir (EST Agadir), in 2006. He received his BSc degree in physics and a post graduate degree in Materials Engineering and energetic environment from Ibn Zohr University, in 2010 and 2012. His research, in the context of national doctoral thesis, focuses on the thematic of Renewable Energies. The doctoral investigation took place in the Research Team in advanced Technologies and Engineering of Renewable Energies (ERTAIER) Agadir Morocco



Lahoussine Bouhouch Professor of higher education at the ESTA (High School of Technologies of Agadir), IbnZohr University, Agadir, Morocco. PhD Electrical Engineering at the Nancy I University, France in 1988 and state doctorate in Electrical in 2007. Responsible of the research team ERTAIR (Research Team in Advanced Technologies and Engineering of Renewable Energies). His research focuses on topics related to renewable energy, instrumentation and electromagnetic compatibility (EMC)



Ahmed Ihlal, was born and brought up in Morocco. He studied Physics and Chemistry and holds, in 1984, his BSc degree (LicenceEs-Sciences Physique) in Solid State Physics from the University Mohamed V, Rabat - Morocco. He then joined Paris VII University – France, where he got, in 1985, a MSc. degree (DEA: Diplome des Etudes Approfondies) in Solar Energy. He pursued his research on the studies and got, in 1988, a PhD degree from the University of Caen BasseNormandie - France. Dr. A. Ihlal started his teaching career on 1988 as Assistant Professor in the faculty of Science at University Ibn Zohr. Then he holds a "Doctorat d'Etat" thesis in 1995. He is currently Full Professor in Faculty of Sciences, University Ibn Zohr, Agadir - Morocco. He is head of the group working on developing cost effective processes for the

fabrication of CIGS and CZTS absorber layers, buffer layers and TCOs. He is working on PV and CSP systems as well. He has published 60 scientific papers, and acted as a referee for numerous international journals. He has contributed to the organization of numerous national and international conferences and was a member of scientific committees for several international conferences. He is supervising PhD, MSc as well as BSc students in the field of PV and CSP. He is an expert of the CNRST in the field of renewable energies.